Nucleophilic Addition to Olefins. 7.[1] Kinetic Deuterium Isotope Effects as Criterion for an Enforced Preassociation Mechanism in the Hydrolysis of Substituted Benzylidene Meldrum's Acids

Claude F. Bernasconi* and Gianni D. Leonarduzzi

Contribution from the Thimann Laboratories of the University of California, Santa Cruz, California 95064. *Received November 13, 1981*

Abstract: The hydrolysis of the title compounds occurs in four steps: (1) nucleophilic attack by water or hydroxide ion to form the addition complex T_{OH}^-; (2) carbon protonation of T_{OH}^- to form T_{OH}^0; (3) oxygen deprotonation of T_{OH}^0 to form T_{OH}^{0-}; (4) collapse of the tetrahedral intermediate T_{OH}^{0-} into the respective benzaldehyde and Meldrum's acid anion. There is also a water-catalyzed collapse of T_{OH}^0 which becomes dominant in strongly acidic solution. In basic solution carbon protonation of T_{OH}^- (step 2) is rate limiting; in strongly acidic media the water-catalyzed collapse of T_{OH}^0 is rate limiting for all substrates. In moderately acidic solution two types of behavior were observed. With the *p*-nitro derivative step 4 is rate limiting at high, step 3 at low buffer concentrations. The latter situation is equivalent to a diffusion-controlled trapping mechanism in the reverse direction. With the parent and the *p*-methoxy derivative, collapse of T_{OH}^{0-} occurs before the protonated base catalyst generated in step 3 can diffuse away; this is equivalent to an enforced preassociation mechanism in the reverse direction and is analogous to the reaction of thiol anions with acetaldehyde studied by Gilbert and Jencks. Our interpretation is strongly supported by (1) α secondary kinetic deuterium isotope effects which are large for the preassociation mechanism but essentially nil for the trapping mechanism and (2) by Brønsted β values around 0.8 in the case of preassociation mechanism and 1.0 for the trapping mechanism. Rate constants for the diffusional separation of the catalyst from T_{OH}^{0-} and for the collapse of the liberated and nonliberated T_{OH}^{0-} species were estimated based on the experimental rate constants and the Hine equation. These calculations show that the main reason for the change in mechanism is the shortened lifetime of the tetrahedral intermediate T_{OH}^{0-} brought about by its destabilization with less electron-withdrawing phenyl substituents. A contributing factor is the slight reduction in the rate of diffusional separation of the catalyst from T_{OH}^{0-} due to the stronger hydrogen bond to the increasingly more basic oxygen in T_{OH}^{0-}. The mechanism for the water-catalyzed collapse of T_{OH}^0 is probably concerted, a conclusion which is supported by a large positive deviation from the Brønsted plot for base catalysis and by a large α secondary kinetic deuterium isotope effect. Rates of carbon protonation of T_{OH}^- (step 2) derived from the parent were determined for a number of acids. These rates show that the intramolecular proton switch, $T_{OH}^- \rightarrow T_{OH}^{0-}$, is *not* a significant pathway.

The hydrolytic cleavage of activated olefins typically involves the four steps shown in eq 1–4 where a and/or b are (is an)

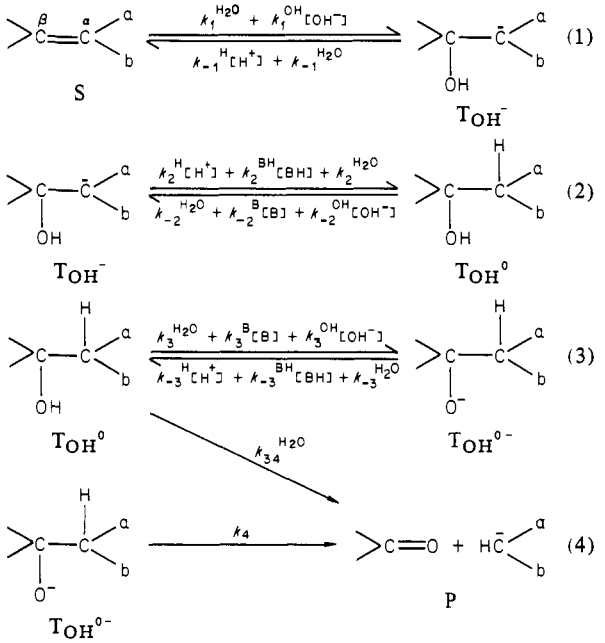

electron-withdrawing substituent(s).[2] The $k_{34}^{H_2O}$ step implies the possibility of a concerted reaction, with water acting as base catalyst; alternative mechanisms for the $k_{34}^{H_2O}$ step will be discussed below. We recently reported a detailed analysis of these four steps in the hydrolysis of benzylidene Meldrum's acid, **1**-H.[3]

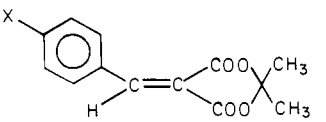

1-H (X = H)
1-OMe (X = OMe)
1-NO_2 (X = NO_2)

We were able (a) to determine $k_1^{H_2O}$, k_1^{OH}, k_{-1}^{H}, $k_{-1}^{H_2O}$, k_2^{H}, k_2^{BH} (BH = $ClCH_2COOH$), $k_{-2}^{H_2O}$, k_{-2}^{B} (B^- = $ClCH_2COO^-$), k_3^{B} (B^- = AcO^-, $HCOO^-$), k_3^{OH}, and $k_{34}^{H_2O}$; (b) to estimate $k_3^{H_2O}$, k_{-3}^{H}, $k_{-3}^{H_2O}$, and k_{-3}^{BH} (BH = AcOH, HCOOH); and (c) to set a lower limit of 10^{10} s^{-1} for k_4.

Since most organic chemists generally consider carbanions to be sluggish nucleofuges, the high rate for the k_4 step was a surprising result. It was partially rationalized by the high stability of the carbanion formed (pK_a of Meldrum's acid is 4.83[4]); it is consistent with similar unpublished observations by Jencks[5] and with a recent report[6] from our laboratory for the reaction

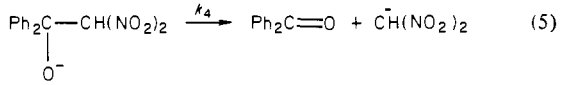

(1) Part 6: Bernasconi, C. F.; Leonarduzzi, G. D. *J. Am. Chem. Soc.*, preceding article in this issue.

(2) For reviews: (a) Patai, S.; Rappoport, Z. In "The Chemistry of Alkenes"; Patai, S., Ed.; Wiley-Interscience: New York, 1964; p 469. (b) Fyfe, C. A. In "The Chemistry of the Hydroxyl Group"; Patai, S., Ed.; Wiley-Interscience: New York, 1971; p 51.

(3) Bernasconi, C. F.; Leonarduzzi, G. D. *J. Am. Chem. Soc.* **1980**, *102*, 1361.

(4) Eigen, M.; Ilgenfritz, G.; Kruse, W. *Chem. Ber.* **1965**, *98*, 1623.

(5) Jencks, W. P. *Acc. Chem. Res.* **1976**, *9*, 475.

(6) Bernasconi, C. F.; Carrē, D. J.; Kanavarioti, A. *J. Am. Chem. Soc.* **1981**, *103*, 4850.

0002-7863/82/1504-5143$01.25/0

Scheme I

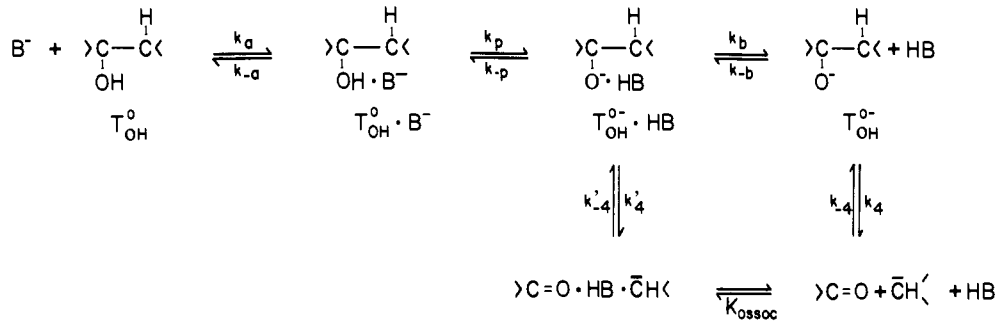

A value of $\geq 10^{10}$ s^{-1} implies that k_4 is of the same order of magnitude as the rate of diffusional separation of two molecules in solution, especially if these two molecules undergo some attractive interaction such as hydrogen bonding which can reduce their rate of separation from its maximum value of $\approx 10^{12}$.[7] This raises some interesting mechanistic questions which are most conveniently discussed with reference to Scheme I.

Scheme I is a more detailed representation of steps 3 and 4 for the base-catalyzed pathways (B = buffer base or OH^-). It shows the diffusional steps involved in the proton transfer according to Eigen[8] (k_a: diffusional encounter; k_p: proton transfer; k_b: diffusional separation). It also shows an additional pathway (k_4') which bypasses the k_b and k_4 steps. This pathway becomes important when $k_4' > k_b$, i.e., when the collapse of T_{OH}^{0-}·HB becomes faster than the diffusional separation between T_{OH}^{0-} and HB. Since such a situation implies that in the reverse direction the reaction has to proceed by the K_{assoc}–k_{-4}' route, this is known as the "preassociation mechanism".[5,9] Examples of acid–base catalyzed reactions which have been shown to proceed by a preassociation mechanism include carbinolamine formation from substituted benzaldehydes,[10,11] the addition of thiol anions to acetaldehyde,[12] the reaction of semicarbazide with 4-methoxyphenyl formate,[13] the addition of certain amines to formaldehyde,[14] the oxidation of methionine by iodine,[15] the decomposition of nitramide,[16] and the reaction of methoxyamine with phenyl acetate.[17]

Our previous study[3] was somewhat inconclusive as to whether the preassociation mechanism prevails in the benzylidene Meldrum's acid system. The major purpose of the present work was to find compelling evidence for or against such a mechanism. To this end we studied the hydrolysis of *p*-methoxy- and *p*-nitrobenzylidene Meldrum's acid (**1-OMe**, **1-NO$_2$**) and also determined α secondary kinetic deuterium isotope effects (D on β carbon) for the hydrolysis of **1-H**, **1-OMe**, and **1-NO$_2$**. Ortiz and Cordes[13] have been the first to use such isotope effects as a probe for a preassociation mechanism in the acid-catalyzed addition of semicarbazide to 4-methoxyphenyl formate.

We also report some hitherto unpublished data on **1-H** which bear on the question as to whether the intramolecular proton switch, $T_{OH}^- \rightarrow T_{OH}^{0-}$, is a significant pathway or not.

It should perhaps be mentioned that our conclusions regarding what are the rate-limiting steps under different reaction conditions are quite different from those drawn by Margaretha et al.[18] based on a more limited set of data in 10% methanol.

Table I. Equilibrium Isotope Effects on Water Addition to Olefins (Eq 6)[a] at 25 °C[b]

				1-NO$_2$			
pH	3.00	3.30	3.40	3.50	3.70		
pK_1^H	3.48	3.52	3.51	3.50	3.41		av 3.484 ± 0.044
pK_1^D	3.46	3.49	3.45	3.43	3.39		av 3.444 ± 0.037
$pK_1^H - pK_1^D$	0.02	0.03	0.06	0.07	0.02		av 0.040 ± 0.021
K_1^H/K_1^D							av 0.912 ± 0.044
				1-H			
pH	5.00	5.30	5.40	5.60	5.70	6.00	
pK_1^H	5.34	5.35	5.34	5.41	5.39	5.40	av 5.372 ± 0.032
pK_1^D	5.31	5.32	5.31	5.36	5.37	5.36	av 5.338 ± 0.028
$pK_1^H - pK_1^D$	0.03	0.03	0.03	0.05	0.02	0.04	av 0.033 ± 0.010
K_1^H/K_1^D							av 0.927 ± 0.021
				1-OMe			
pH	6.00	6.30	6.40	6.50	6.70		
pK_1^H	6.58	6.56	6.58	6.59	6.65		av 6.592 ± 0.034
pK_1^D	6.54	6.54	6.56	6.57	6.63		av 6.568 ± 0.037
$pK_1^H - pK_1^D$	0.04	0.02	0.02	0.02	0.02		av 0.024 ± 0.009
K_1^H/K_1^D							av 0.946 ± 0.020

[a] Defined in terms of $[H^+]$, see ref 19. Error limits are standard deviations. [b] μ = 0.5 M.

Results

Equilibrium Isotope Effect on Step 1. The equilibrium for water addition to the olefins (eq 1) corresponds to a pseudo-acid–base equilibrium as shown in eq 6. K_1 had already been measured

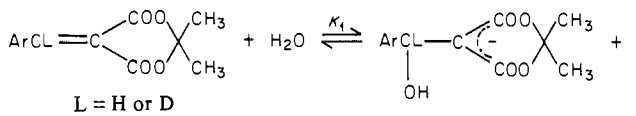

L = H or D

T_{OH}^-

H_3O^+ (6)

kinetically for **1-H**,[3] **1-OMe**,[1] and **1-NO$_2$**.[1] However, in order to determine the secondary deuterium isotope effect on K_1, new measurements were performed, mostly by a standard spectrophotometric technique, but also some by kinetics.

Special care was taken in achieving good precision in the isotope effects. Thus, any given spectrophotometric determination was always carried out simultaneously for both the protio and respective deuterio compound, using identical buffer solutions. Nevertheless, the reproducibility of the isotope effects was somewhat disappointing as the data summarized in Table I[19] show. The major problem was that the solutions were not stable because of the hydrolysis reaction. Hence OD readings had to be taken as a function of time and the OD at time zero was determined by extrapolation (for details, see Experimental Section). For **1-H** and **1-NO$_2$** the extrapolated OD differed by less than 10% from the first OD reading after mixing (20 s after mixing), and therefore

(7) For some leading references, see: Murdoch, J. R. *J. Am. Chem. Soc.* **1980**, *102*, 71.
(8) Eigen, M. *Angew. Chem., Int. Ed. Engl.* **1964**, *3*, 1.
(9) Jencks, W. P. *Acc. Chem. Res.* **1980**, *13*, 161.
(10) Sayer, J. M.; Jencks, W. P. *J. Am. Chem. Soc.* **1973**, *95*, 5637.
(11) Sayer, J. M.; Edman, C. *J. Am. Chem. Soc.* **1979**, *101*, 3010.
(12) (a) Gilbert, H. F.; Jencks, W. P. *J. Am. Chem. Soc.* **1977**, *99*, 7931. (b) Jencks, W. P.; Gilbert, H. F. *Pure Appl. Chem.* **1977**, *49*, 1021.
(13) Ortiz, J. J.; Cordes, E. H. *J. Am. Chem. Soc.* **1978**, *100*, 7080.
(14) Abrams, W. R.; Kallen, R. G. *J. Am. Chem. Soc.* **1976**, *98*, 7777.
(15) Young, P. R.; Hsieh, L.-S. *J. Am. Chem. Soc.* **1978**, *100*, 7121.
(16) (a) Kresge, A. J.; Tang, Y. C. *J. Chem. Soc., Chem. Commun.* **1980**, 309. (b) Kresge, A. J. *Pure Appl. Chem.* **1981**, *53*, 189.
(17) Jencks, W. P.; Cox, M. M. *J. Am. Chem. Soc.* **1981**, *103*, 572.
(18) Margaretha, P.; Schuster, P.; Polansky, O. E. *Tetrahedron* **1971**, *27*, 71.

(19) $[H^+] = a_{H^+}/\gamma_{H^+}$ where a_{H^+} is the activity measured with the glass electrode and γ_{H^+} = 0.74 at μ = 0.5 M: Harned, H. S.; Robinson, R. A. In "Multicomponent Electrolyte Solutions"; Pergamon Press, Elmsford, N.Y., 1968; p 50.

Table II. α Secondary Kinetic Deuterium Isotope Effects on the Water Addition to 1-OMe and 1-NO_2 at 25 °C[a,b]

buffer	pH	$(\tau_{OH/H_2O}^{-1})_H$, s^{-1}	$(\tau_{OH/H_2O}^{-1})_D$, s^{-1}	$(k_1^{H_2O})_H/(k_1^{H_2O})_D$	$(k_{-1}^{H})_H/(k_{-1}^{H})_D$
		A. 1-OMe			
AcOH	4.50	13.3	12.8		
		13.4	12.6		
		13.9	13.0		
		av 13.53 ± 0.32	12.80 ± 0.20		1.057 ± 0.025
AcOH	4.52	12.7	12.5		
		12.8	11.7		
		13.0	12.1		
		av 12.83 ± 0.15	12.10 ± 0.40		1.060 ± 0.031
p-CNC_6H_4OH	7.95	0.119	0.142		
		0.122	0.131		
		0.132	0.134		
		0.129	0.137		
		av 0.1255 ± 0.0059	0.1360 ± 0.0047	0.923 ± 0.043	
		B. 1-NO_2			
$H_2PO_4^-$	6.00	1.90	2.07		
		1.95	2.07		
		1.94	2.04		
		av 1.930 ± 0.026	2.060 ± 0.017	0.937 ± 0.013	

[a] Error limits are standard deviations. [b] μ = 0.5 M.

possible errors introduced by this extrapolation are expected to be relatively small. For **1-OMe** hydrolysis was appreciably faster and the extrapolated OD differed by as much as 30% from the first reading, substantially increasing the possibility for error.

The average isotope effects determined spectrophotometrically are K_1^H/K_1^D = 0.912 ± 0.044, 0.927 ± 0.021, and 0.946 ± 0.020 for **1-NO_2**, **1-H**, and **1-OMe**, respectively; the error limits represent standard deviations. In view of the experimental problems mentioned above and since there is no good reason to assume that K_1^H/K_1^D should significantly depend on the phenyl substituent, we believe that the result for **1-OMe** is not very reliable and should probably be discarded. This view is supported by the results of a kinetic determination of the isotope effect. The general kinetic behavior of reaction 1 was investigated thoroughly before.[1] The reciprocal relaxation time, τ_{OH/H_2O}^{-1} for equilibrium approach is given by[20]

$$\tau_{OH/H_2O}^{-1} = k_1^{H_2O} + k_1^{OH}[OH^-] + k_{-1}^{H}[H^+] + k_{-1}^{H_2O} \quad (7)$$

In Table II isotope effects on τ_{OH/H_2O}^{-1} are reported as measured by the stopped-flow method. At pH 4.50 and 4.52 the k_{-1}^{H}-$[H^+]$-term of eq 7 is dominant in the reaction of **1-OMe**[1] and hence $(\tau_{OH/H_2O}^{-1})_H/(\tau_{OH/H_2O}^{-1})_D = (k_{-1}^{H})_H/(k_{-1}^{H})_D$. These ratios are 1.057 ± 0.025 and 1.060 ± 0.031 at pH 4.50 and 4.52, respectively.

At pH 7.95 it is the $k_1^{H_2O}$ term which dominates τ_{OH/H_2O}^{-1} and $(\tau_{OH/H_2O}^{-1})_H/(\tau_{OH/H_2O}^{-1})_D = (k_1^{H_2O})_H/(k_1^{H_2O})_D$ = 0.923 ± 0.043. In view of the rather large standard deviation which is probably due to an instrument problem in that time range, we also determined the isotope effect on $k_1^{H_2O}$ for **1-NO_2** which is most conveniently done at pH 6.00.[1] The scatter in the data is much smaller than for **1-OMe** (Table II) but the resulting $(k_1^{H_2O})_H/(k_1^{H_2O})_D$ = 0.937 ± 0.013 is very similar to that found for **1-OMe**.

In calculating the equilibrium isotope effect, K_1^H/K_1^D = 0.906, we took the average of three K_1^H/K_1^D ratios: the spectrophotometric ratios for **1-NO_2** and **1-H** and the average of the kinetically determined ones.

Rates of Hydrolysis. Rates of the overall reaction (S in eq 1 to P in eq 4) were measured in a variety of buffers by a conventional spectrophotometric technique. At pH ≤ pK_1 the reaction was monitored by following the loss of the olefin, at pH > pK_1 by following the loss of T_{OH}^- which is the new ground state. A number of runs involved the deuterated olefins. Just as for the equilibrium isotope effects, in order to minimize errors, the kinetic isotope effects were determined by concurrent measurements on the protio and deuterio compound, using the same buffer solutions. This necessitated a partial reinvestigation of the previously reported[3] hydrolysis of **1-H**. Some data in basic solution (morpholine, carbonate, and triethylamine buffers) not previously reported for **1-H** are also included in the present study.

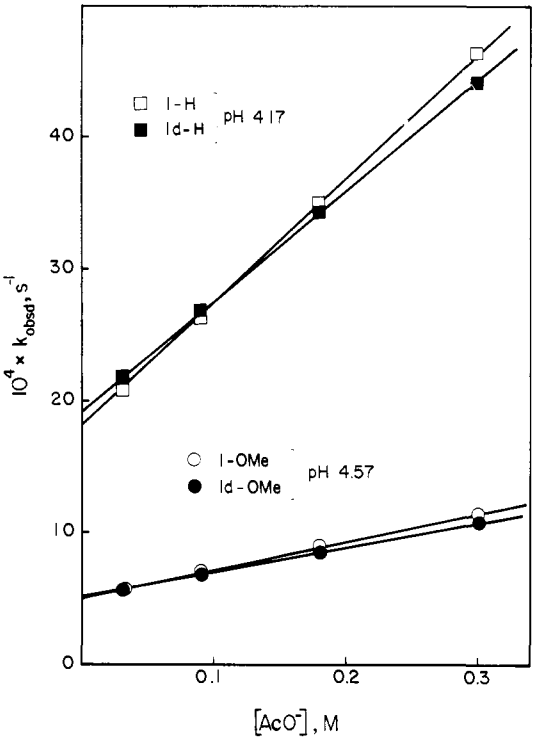

Figure 1. Observed rate constants for hydrolysis of 1-H and **1-OMe** and their deuterated analogues in acetate buffers (data from Tables S2 and S3[21]).

The results of the pairwise experiments involving the protio and deuterio substrates are summarized in Tables S1–S3[21] (116 rate constants). For **1-NO_2** they refer to HCl solutions (pH 1.00, 1.30, 1.50), to formate buffers (pH 3.00), and to acetate buffers (pH 4.10 and 4.50); for **1-H** to formate buffers (pH 3.47) and acetate buffers (pH 4.17 and 4.57); for **1-OMe** to formate buffers (pH 3.46) and acetate buffers (pH 4.57 and 4.97). Additional results with the protio substrates only are in Table S4[21] (82 rate constants). They include data in chloroacetate, methoxyacetate, formate, morpholine, bicarbonate, and triethylamine buffers.

Figures 1–3 show representative plots of k_{obsd} vs. the concentration of the buffer base. Three types of buffer plots were

(20) Equation 7 holds at low buffer concentration; at high buffer concentration terms for buffer catalysis need to be included for **1-OMe**.[1]

(21) See paragraph concerning supplementary material at the end of this paper.

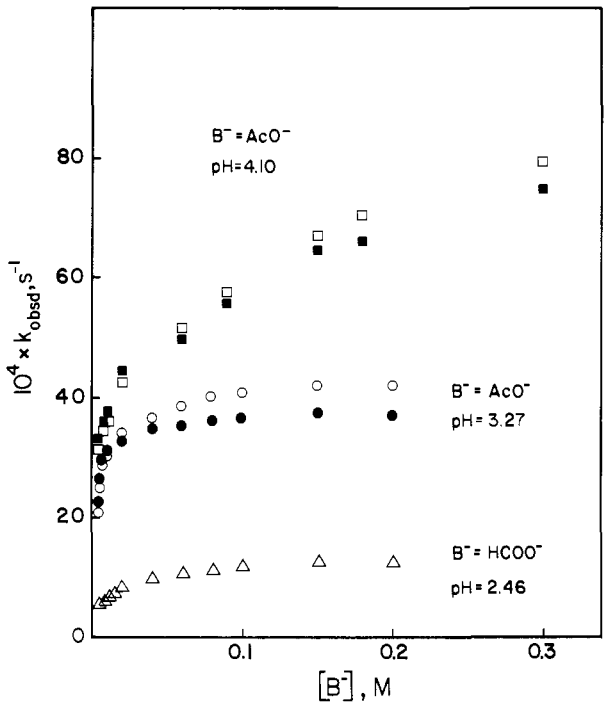

Figure 2. Observed rate constants for hydrolysis of 1-NO_2 and 1d-NO_2 in acetate and formate buffers (data from Tables S1 and S4[21]). Open symbols, 1-NO_2; filled symbols, 1d-NO_2.

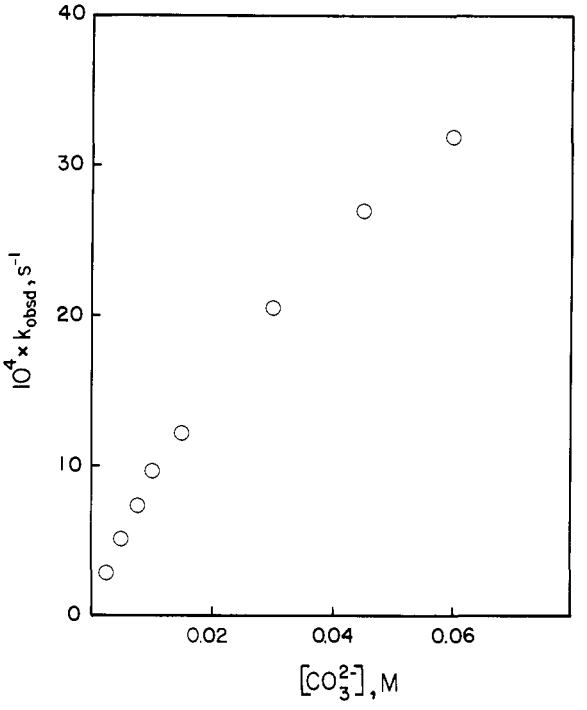

Figure 3. Observed rate constants for hydrolysis of 1-H in a carbonate buffer at pH 9.93 (data from Table S4[21]).

observed. The first type shows a linear dependence (Figure 1) as exemplified by acetate catalysis of the reactions of **1-H** and **1-OMe**. The second is a nonlinear dependence as observed for acetate and formate catalysis of the reaction of **1-NO_2** (Figure 2). The third, shown in Figure 3 for the reaction of **1-H** in carbonate buffers, appears at first sight to be similar to the second. However the extent of carbonate catalysis is very much greater (60-fold rate increase for a 0.06 M concentration) than that found for acetate or formate catalysis in either Figure 1 or 2 (2- to 2.5-fold increase in 0.3 M solutions). This suggests that carbonate catalysis has a different mechanistic origin as will be borne out by the analysis presented in the Discussion.

Table III. Equilibrium Constant for Steps 1 and 2 at 25 °C and μ = 0.5 M[a]

	1-OMe	1-H	1-NO_2
K_1	3.33×10^{-7}	3.75×10^{-6}	3.43×10^{-4}
pK_1	6.48	5.43	3.46
K_a^{CH}	5.13×10^{-4}	1.12×10^{-3}	9.23×10^{-3}
pK_a^{CH}	3.29	2.95	2.04

[a] From ref 1 and 3.

The results show that the deuterio substrates react somewhat more slowly than the protio compounds at high buffer concentrations while the opposite is true at low buffer concentrations.

Discussion

Mechanism of Hydrolysis in Acidic Solution. 1-NO_2. We shall first discuss **1-NO_2** with reference to eq 1–4. Our previous work demonstrated that steps 1 and 2 are quite fast compared to the rate of the overall hydrolysis.[1,3] Hence we can treat these steps as rapid preequilibria and, since T_{OH}^{0-} can never accumulate and is therefore a steady-state intermediate in acidic solution, k_{obsd} is given by[19,22]

$$k_{obsd} = \frac{K_1[H^+]}{K_1[H^+] + K_a^{CH}[H^+] + K_a^{CH}K_1} \times \left\{ \frac{(k_3^{H_2O} + k_3^{B}[B] + k_3^{OH}[OH^-])k_4}{k_4 + k_{-3}^{H}[H^+] + k_{-3}^{BH}[BH] + k_{-3}^{H_2O}} + k_{34}^{H_2O} \right\} \quad (8)$$

K_a^{CH} is the C–H acidity constant of T_{OH}^{0}. In order to facilitate the discussion the values of K_1 and K_a^{CH} are summarized in Table III.

Since for all substrates $K_a^{CH} \gg K_1$ eq 8 simplifies to

$$k_{obsd} = \frac{K_1}{K_1 + [H^+]} \times \frac{[H^+]}{K_a^{CH}} \left\{ \frac{(k_3^{H_2O} + k_3^{B}[B] + k_3^{OH}[OH^-])k_4}{k_4 + k_{-3}^{H}[H^+] + k_{-3}^{BH}[BH] + k_{-3}^{H_2O}} + k_{34}^{H_2O} \right\} \quad (9)$$

The curvature in the buffer plots (Figure 2) indicates a change in the rate-limiting step. The linearity[24] at low concentration implies $k_4 \gg k_{-3}^{H}[H^+] + k_{-3}^{BH}[BH] + k_{-3}^{H_2O}$ so that eq 9 reduces to

$$k_{obsd} = \frac{K_1}{K_1 + [H^+]} \frac{[H^+]}{K_a^{CH}} (k_3^{H_2O} + k_{34}^{H_2O} + k_3^{B}[B] + k_3^{OH}[OH^-]) \quad (10)$$

I.e., oxygen deprotonation of T_{OH}^{0} ("trapping mechanism"[25]) is rate limiting, along with a possible concurrent concerted pathway ($k_{34}^{H_2O}$). At high concentration we have $k_4 \ll k_{-3}^{BH}[BH] + k_{-3}^{H}[H^+] + k_{-3}^{H_2O}$, and eq 9 becomes

$$k_{obsd} = \frac{K_1}{(K_1 + [H^+])K_a^{CH}} (K_a^{OH}k_4 + k_{34}^{H_2O}[H^+]) \quad (11)$$

K_a^{OH} is the O–H acidity constant of T_{OH}^{0}. Here collapse of T_{OH}^{0-} (k_4 pathway) is rate limiting, again in possible competition with the $k_{34}^{H_2O}$ pathway.

This interpretation is borne out by the following numerical analysis: k_3^{B} is obtained from the *initial* slopes (Figure 2) via eq 10 while $k_{3'}^{H_2O} + k_3^{OH}[OH^-]$ (where $k_{3'}^{H_2O} = k_3^{H_2O} + k_{34}^{H_2O}$)

(22) $[OH^-]$ was calculated as $[OH^-] = K_w/[H^+]$ with $K_w = 1.87 \times 10^{-14}$ at μ = 0.5 M[23] and $[H^+]$ according to ref 19.

(23) Harned, H. S.; Owen, B. B. "The Physical Chemistry of Electrolyte Solutions"; Reinhold: New York, 1950; p 487.

(24) Strictly speaking the linearity only implies $k_4 >> k_{-3}^{BH}[BH]$. However, subsequent analysis will show that the $k_{-3}^{H}[H^+]$ term is negligible compared to $k_{-3}^{H_2O}$ at the pH values used, and that $k_4 >> k_{-3}^{H_2O}$ is a fairly good approximation.

(25) This is called the trapping mechanism[5,9] because in the reverse direction T_{OH}^{0-} is trapped by encounter-controlled protonation (k_{-b}-step in Scheme I).

Table IV. Rate Constants for Steps 3 and 4[a] at 25 °C and μ = 0.5 M

constant[b]	pK_a^{BH}	1-OMe (pK_a^{OH} = 14.7)	1-H (pK_a^{OH} = 14.45)	1-NO_2 (pK_a^{OH} = 13.65)
$k_3^{H_2O}/[H_2O]$[c]	−1.74	$3.54 \times 10^{-1}/55$	$1.60 \times 10^{-1}/55$	$8.70 \times 10^{-3}/55$
$k_3^{ClCH_2COO^-}$	2.65			7.48×10^{-2}
$k_{-3}^{ClCH_2COOH}$	2.65			$\approx 10^{10}$
$k_3^{HCOO^-}$	3.46	3.31×10^{-1}	3.32×10^{-1}	4.96×10^{-1}
k_{-3}^{HCOOH}	3.46			$\approx 10^{10}$
$k_3^{MeOCH_2COO^-}$	3.48	3.11×10^{-1}		
$k_{-3}^{MeOCH_2COOH}$	3.48			
$k_3^{AcO^-}$	4.57	2.31	2.82	8.29
k_{-3}^{AcOH}	4.57			$\approx 10^{10}$
k_3^{OH}	15.47[d]	9.40×10^8	1.70×10^9	1.80×10^9
$k_{-3}^{H_2O}/[H_2O]$	15.47[d]			$1.50 \times 10^9/55$
k_4				5.40×10^9

[a] Defined in terms of $[H^+]$ and $[OH^-]$; see ref 19 and 22. [b] Units of M^{-1} s^{-1}. [c] $k_{3'}^{H_2O} = k_3^{H_2O} + k_{34}^{H_2O}$. [d] pK_w + log $[H_2O]$ with pK_w = 13.73 at μ = 0.5 M (ref 22).

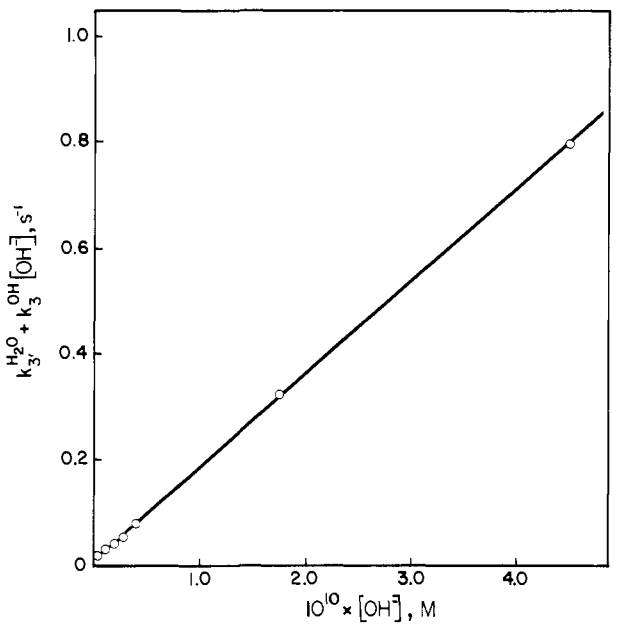

Figure 4. Plot of $k_{3'}^{H_2O} + k_3^{OH}[OH^-]$ vs. $[OH^-]$ for 1-NO_2; $k_{3'}^{H_2O} + k_3^{OH}[OH^-]$ obtained, via eq 10, from intercepts of buffer plots.

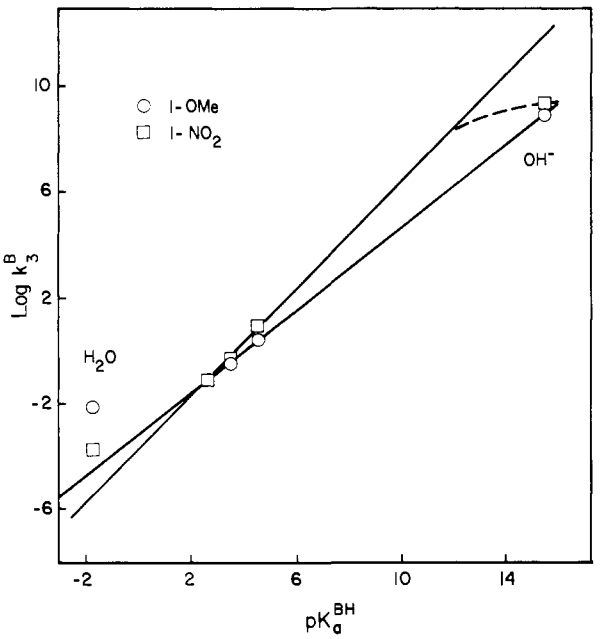

Figure 5. Brønsted plot for general base catalysis of conversion of T_{OH}^0 into Meldrum's acid anion and the corresponding substituted benzaldehyde. For 1-NO_2 the plot corresponds to an Eigen curve with β = 1.00 for thermodynamically unfavorable proton transfer and encounter-controlled rate for thermodynamically favorable proton transfer (B^- = OH^-). For 1-OMe β = 0.81 which is characteristic of a preassociation mechanism.

is obtained from the intercepts, again via eq 10. A plot of $k_{3'}^{H_2O} + k_3^{OH}[OH^-]$ vs. $[OH]$[22] is shown in Figure 4 from which k_3^{OH} = 1.8×10^9 M^{-1} s^{-1} is calculated. $k_{3'}^{H_2O}$ is too small to be determined very accurately from Figure 4, but it is obtained from experiments in HCl solution at pH ≤2.0 where $k_3^{OH}[OH^-]$ is negligible. The various rate constants are summarized in Table IV. A Brønsted plot is shown in Figure 5. The slope defined by the three carboxylate ions affords β = 1.00 ± 0.05 while the point for hydroxide ion deviates negatively by 2.6 log units. This is the typical behavior for proton transfers between two oxygens where β is unity and diffusional separation (k_b in Scheme I) is rate limiting in the thermodynamically unfavorable direction, while k_3^{OH} has a value (1.8×10^9 M^{-1} s^{-1}) which approaches that for a thermodynamically favorable encounter controlled reaction.[8] The pK_a^{OH} of the OH group of T_{OH}^0 can be estimated as $K_a^{OH} = K_a^{BH} k_3^B / k_{-3}^{BH} \approx 2.2 \times 10^{-14}$ ($pK_a^{OH} \approx 13.65$) by assuming $k_{-3}^{BH} \approx 10^{10}$ M^{-1} s^{-1}.[8] This pK_a^{OH} value shows that deprotonation by OH^- is indeed thermodynamically somewhat favored (ΔpK = 15.47 − 13.65 = 1.82), consistent with the high k_3^{OH} value. Nevertheless, we note that k_3^{OH} is not quite as high ($\approx 10^{10}$ M^{-1} s^{-1}) as commonly observed for encounter-controlled deprotonations by OH^-. This suggests that the actual proton transfer step (k_p in Scheme I) could be partially rate limiting, owing to the small ΔpK.

The point for the water reaction(s) ($k_{3'}^{H_2O}$) is seen to deviate positively from the Brønsted plot by ≈1.8 log units. This deviation indicates that $k_{34}^{H_2O}$ must be dominant as discussed in more detail below.

From the plateau at pH 3.27 (Figure 2) one calculates, via eq 11, $K_a^{OH}k_4 + k_{34}^{H_2O}[H^+] = 1.21 \times 10^{-4}$. Since we concluded above that $k_{3'}^{H_2O} \approx k_{34}^{H_2O}$ we have $k_{34}^{H_2O}[H^+] \approx 6.3 \times 10^{-6}$ at this pH; thus we obtain $K_4^{OH}k_4 = 1.15 \times 10^{-4}$ and hence k_4 = 5.13×10^9 s^{-1}. At pH 2.46 the plateau yields $K_a^{OH}k_4 + k_{34}^{H_2O}[H^+]$ = 1.68×10^{-4} while $k_{34}^{H_2O}[H^+] = 4.1 \times 10^{-5}$. This leads to k_4 = 5.67×10^9 s^{-1}. We shall adopt the average of 5.40×10^9 s^{-1} for k_4. We see now that the assumption[24] that $k_4 >> k_{-3}^{H_2O}$ = 1.5×10^9 (from k_3^{OH} and pK_a^{OH}) is a fairly good one.

1-OMe and 1-H. In the hydrolysis of **1-OMe** there is no curvature in the buffer plots (Figure 1), implying that eq 10 is valid at all concentrations. This is the same behavior found earlier for **1-H**.[3] Analysis of the data affords the rate constants summarized in Table IV; they are displayed on a Brønsted plot in Figure 5. Since catalysis by chloroacetate buffer was too weak to yield a reliable k_3^B value, β for the carboxylate ions was reckoned as β = log $(k_3^{AcO^-}/k_3^{MeOCH_2COO^-})/(pK_a^{AcOH} - pK_a^{MeOCH_2COOH})$ = 0.81. This value is significantly lower than β = 1.00 for 1-NO_2 but similar to β = 0.83 for **1-H**.[3] In view of the small number of suitable catalysts available for evaluating the Brønsted slopes the reported β values may be somewhat uncertain. However, the important point here is not so much the precise value of β but the fact that β for **1-OMe** and **1-H** is

Table V. α Secondary Kinetic Deuterium Isotope Effects on Hydrolysis Reaction at 25 °C and μ = 0.5 M

buffer	pH	obsd quantity[a]		derived quantity[b]		mechanistic interpretation
				A. 1-NO_2		
AcO^-	3.27	k_{obsd}^H/k_{obsd}^D	1.130	$(k_4)_H/(k_4)_D$	1.20	$(k_4)_H/(k_4)_D$
AcO^-	4.50	slope^H/slope^D	1.003	$(k_3^B)_H/(k_3^B)_D$	1.06	$(K_a^{OH})_H/(K_a^{OH})_D = 1.05$
	4.10		0.995		1.07	
	3.27		0.958		1.07	
$HCOO^-$	3.00		0.961		1.09	
AcO^-	4.50		0.953	$(k_3^{OH})_H/(k_3^{OH})_D$	1.01	$(k_a)_H/(k_a)_D = 1.00$
	4.10		0.949		1.02	
	3.27		0.927	$\frac{(k_{34}^{H_2O} + k_3^{OH}[OH^-])_H}{(k_{34}^{H_2O} + k_3^{OH}[OH^-])_D}$	1.04	see text
$HCOO^-$	3.00	int^H/int^D	0.933		1.06	
HCl	1.50		1.100	$(k_{34}^{H_2O})_H/(k_{34}^{H_2O})_D$	1.27	$(k_{34}^{H_2O})_H/(k_{34}^{H_2O})_D$
	1.30		1.110		1.29	
	1.00		1.105		1.28	
				B. 1-H		
AcO^-	4.57	slope^H/slope^D	1.135	$(k_3^B)_H/(k_3^B)_D$	1.30	$\frac{(K_a^{OH})_H}{(K_a^{OH})_D}\frac{(k_4')_H}{(k_4')_D} = 1.05\frac{(k_4')_H}{(k_4')_D}$
	4.17		1.30		1.30	
$HCOO^-$	3.46		1.126		1.30	
AcO^-	4.57	int^H/int^D	0.930	$\frac{(k_{34}^{H_2O} + k_3^{OH}[OH^-])_H}{(k_{34}^{H_2O} + k_3^{OH}[OH^-])_D}$	1.07	see text[c]
	4.17		0.948		1.09	
$HCOO^-$	3.46		1.025		1.19	
				C. 1-OMe		
AcO^-	4.97	slope^H/slope^D	1.136	$(k_3^B)_H/(k_3^B)_D$	1.31	$\frac{(K_a^{OH})_H}{(K_a^{OH})_D}\frac{(k_4')_H}{(k_4')_D} = 1.05\frac{(k_4')_H}{(k_4')_D}$
	4.57		1.140		1.32	
$HCOO^-$	3.46		1.165		1.35	
AcO^-	4.97	int^H/int^D	0.930	$\frac{(k_{34}^{H_2O} + k_3^{OH}[OH^-])_H}{(k_{34}^{H_2O} + k_3^{OH}[OH^-])_D}$	1.08	see text[d]
	4.57		0.977		1.13	
$HCOO^-$	3.46		1.070		1.24	

[a] Estimated error ±0.015. [b] Estimated error ±0.03 to ±0.04; the error in the derived quantities is higher than for the observed quantities because it includes errors in K_1^H/K_1^D and potential errors in the estimated $(K_a^{CH})_H/(K_a^{CH})_D$. [c] $(k_{34}^{H_2O})_H/(k_{34}^{H_2O})_D = 1.26$, $(k_3^{OH})_H/(k_3^{OH})_D = 1.03$ obtained as described in the text. [d] $(k_{34}^{H_2O})_H/(k_{34}^{H_2O})_D = 1.24$, $(k_3^{OH})_H/(k_3^{OH})_D = 1.03$ obtained as described in the text.

significantly different from β for **1-NO_2**. That this is indeed the case can also be appreciated by comparing the $k_3^{AcO^-}/k_3^{HCOO^-}$ ratios which are similar for **1-OMe** (6.98) and **1-H** (8.48), but quite different (16.7) for **1-NO_2**.

The point for $k_3^{OH} = 9.40 \times 10^8\ M^{-1}\ s^{-1}$ is also lower than for **1-NO_2** and lies approximately on the Brønsted line defined by the carboxylate ions; the point for the water reaction deviates positively by a factor of about 400.

One possible interpretation of these results is that **1-OMe** (and **1-H**) behaves essentially in the same way as **1-NO_2**; the somewhat lower k_3^B and k_3^{OH} values would be consistent with a somewhat higher pK_a^{OH}, estimated to be 14.70 for **1-OMe** and 14.45 for **1-H** by assuming a Hammett ρ value of 1.0.[26] The low Brønsted values for both **1-OMe** and **1-H** would then have to be attributed to experimental error. This is not a satisfactory explanation. A better interpretation is that the reactions follow the preassociation mechanism shown in Scheme I. The following points argue in favor of this interpretation.

(1) Rate-limiting oxygen deprotonation of T_{OH}^0 by a carboxylate ion implies that diffusional separation (k_b step in Scheme I) is rate limiting, with $k_3^B = K_{as}K_pk_b$ where $K_{as} = k_a/k_{-a}$ and $K_p = k_p/k_{-p}$. If the same mechanism were to apply to **1-OMe** and **1-NO_2** the ratios k_3^B(**1-NO_2**)/k_3^B(**1-OMe**) should be given by K_a^{OH}(**1-NO_2**)/K_a^{OH}(**1-OMe**) ≈ 11.2. The experimental k_3^B(**1-NO_2**)/k_3^B(**1-OMe**) ratios are, however, 1.60 for formate ion and 3.58 for acetate ion catalysis. Similar discrepancies between expected and observed ratios exist for **1-H**. These discrepancies are much too large to be accounted for by experimental error.

(2) A Brønsted β value around 0.8 is consistent with the preassociation mechanism.[5,9] In this mechanism the k_4' step (Scheme I) is rate limiting and $k_3^B = K_{as}K_pk_4'$. In as much as the transition state is stabilized by hydrogen bonding from HB to the oxygen in a similar way as the complex T_{OH}^{0-}·HB (Scheme I), this would attenuate the dependence of k_3^B on pK_a^{BH} and would imply weak acid catalysis ($\alpha \approx 0.2$) in the reverse direction. This point will be elaborated upon below.

(3) The most compelling evidence derives from the secondary kinetic deuterium isotope effects.

Evidence from Isotope Effects. The isotope effect data are summarized in Table V; their mechanistic meaning is now discussed. **1-NO_2** has been the most thoroughly studied compound because it provides a "calibration" as to what size of isotope effects should be expected when C–C bond breaking is rate limiting (k_4 or k_4') and when diffusional separation is rate limiting. Such calibration is desirable because for the preequilibrium isotope effects either only estimates are available (K_a^{CH}, K_a^{OH}) or the experimental error is relatively high (K_1); however, all these potential errors are expected to affect each compound similarly.

At high acetate ion concentration, pH 3.27, k_{obsd} reaches a plateau (Figure 2) which is given by eq 11. Earlier we showed that a this pH the $k_{34}^{H_2O}[H^+]$ term only contributes ≈5% to the plateau. Hence, neglecting this term we obtain expression 12 for

$$\frac{(k_4)_H}{(k_4)_D} = \frac{(k_{obsd})_H}{(k_{obsd})_D}\frac{K_1^D(K_1^H + [H^+])}{K_1^H(K_1^D + [H^+])}\frac{(K_a^{CH})_H}{(K_a^{CH})_D}\frac{(K_a^{OH})_D}{(K_a^{OH})_H} \quad (12)$$

the isotope effect on k_4. Using $K_1^H/K_1^D = 0.906$ (see Results) and assuming $(K_a^{CH})_H/(K_a^{CH})_D = (K_a^{OH})_H/(K_a^{OH})_D = 1.05$,[32] one

(26) The ρ value for the pK_a of $ArCH(OH)CF_3$ is 1.01.[27] A different method of estimating pK_a^{OH} of **1-H** is based on a Taft correlation of the form $pK_a = 16.56 - 1.38\ (\sigma^*_{R'} + \sigma^*_{R''} + \sigma^*_{R'''})$ for alcohols of the type R′R″R‴OH.[28] Using 0.6 for σ^*_{Pb},[29] 0.29 for σ^*_H,[28] and 0.75 for σ* of the $CH(COO)_2C(CH_3)_2$[30] group, one obtains $pK_a^{OH} = 14.5$. Our previous estimate of 14.1[3] was based on the assumption of a trapping mechanism which is now discarded.

(27) Stewart, R.; Van der Linde, R. *Can. J. Chem.* **1960**, *38*, 399.

(28) Hine, J. *J. Am. Chem. Soc.* **1971**, *93*, 3701.

(29) Taft, R. W. In "Steric Effects in Organic Chemistry"; Newman, M. S., Ed.; Wiley: New York, 1956; Chapter 13.

(30) σ_1 for $CH(COO)_2C(CH_3)_2$ is assumed to be twice as large as σ_1 = 0.17 for CH_2COOR.[31] σ* is obtained as $\sigma_1/0.45$.[31]

(31) Exner, O. In "Correlation Analysis in Chemistry"; Chapman, N. B.; Shorter, J. Eds.; Plenum: New York, 1978; p 439.

(32) Secondary α-deuterium isotope effects on acidity constants for oxygen and nitrogen acids are generally around 1.05[33] and arise mainly from an apparent electron-donating effect of deuterium.[33,34] In the absence of experimental data we shall assume that the isotope effect on K_a^{CH} is the same.

calculates $(k_4)_H/(k_4)_D = 1.20$. This rather large isotope effect is consistent with what has been observed in other reactions where there is a change from sp^3 to sp^2 carbon;[35-38] its implication regarding transition state structure will be discussed below.

From the data at low buffer concentration one obtains the isotope effect on k_3^B as

$$\frac{(k_3^B)_H}{(k_3^B)_D} = \frac{\text{slope}^H}{\text{slope}^D}\frac{K_1^D(K_1^H + [H^+])}{K_1^H(K_1^D + [H^+])}\frac{(K_a^{CH})_H}{(K_a^{CH})_D} \quad (13)$$

where slope^H and slope^D are the *initial* slopes of k_{obsd}^H and k_{obsd}^D, respectively, vs. buffer base concentration. For acetate ion catalysis we obtain $(k_3^B)_H/(k_3^B)_D = 1.07$, for formate ion catalysis $(k_3^B)_H/(k_3^B)_D = 1.09$; the former value represents the average of three isotope effects determined at three different pH values (Table V).

Diffusional separation (k_b) being rate limiting, the mechanistic meaning of these isotope effects is given by

$$\frac{(k_3^B)_H}{(k_3^B)_D} = \frac{(K_{as}K_pk_b)_H}{(K_{as}K_pk_b)_D} = \frac{(K_a^{OH}/K_a^{BH})_H}{(K_a^{OH}/K_a^{BH})_D} = \frac{(K_a^{OH})_H}{(K_a^{OH})_D} \approx 1.05 \quad (14)$$

The second and third equalities hold because the diffusional steps are not expected to show an isotope effect and K_a^{BH} cannot possibly depend on the isotope in the substrate. The observed values for $(k_3^B)_H/(k_3^B)_D$, particularly the one for formate ion catalysis, are seen to be slightly higher than the value of 1.05 expected for $(K_a^{OH})_H/(K_a^{OH})_D$.[33] This could be due (a) to experimental error in the hydrolysis data, (b) experimental error in K_1^H/K_1^D,[39] (c) a slight overestimate of $(K_a^{CH})_H/(K_a^{CH})_D$ or underestimate of $(K_a^{OH})_H/(K_a^{OH})_D$, (d) a small contribution by the preassociation mechanism (see below), or a combination of any or all of these factors. Be it as it may, the important fact is that $(k_3^B)_H/(k_3^B)_D$ is very close to the expected value of ≈1.05 and is consistent with the trapping mechanism.

From the isotope effects on the intercepts, $(\text{int}^H/\text{int}^D)$ of the buffer plots (or on k_{obsd} determined in HCl solution), one obtains

$$\frac{(k_3^{OH}[OH^-] + k_{34}^{H_2O})_H}{(k_3^{OH}[OH^-] + k_{34}^{H_2O})_D} = \frac{\text{int}^H}{\text{int}^D}\frac{K_1^D(K_1^H + [H^+])}{K_1^H(K_1^D + [H^+])}\frac{(K_a^{CH})_H}{(K_a^{CH})_D} \quad (15)$$

At pH ≥4.10 $k_3^{OH}[OH^-] >> k_{34}^{H_2O}$ and hence eq 15 becomes equivalent to the isotope effect on k_3^{OH}. The experimental values (Table V) are 1.01 (pH 4.57) and 1.02 (pH 4.10). Mechanistically k_3^{OH} corresponds to diffusional encounter or some mixture of diffusional encounter and proton transfer (k_a and k_p in Scheme I) for which an isotope effect of 1.00 is expected. The observed values are in excellent agreement with this expectation.

At pH ≤1.5 it is the $k_{34}^{H_2O}$ term which is dominant in eq 15 and one obtains $(k_{34}^{H_2O})_H/(k_{34}^{H_2O})_D = 1.28$ as the average from three pH values (Table V). This high value, similar to that for the breakdown of T_{OH}^{0-} (k_4) but very different from the isotope effects on the base-catalyzed pathways (k_3^{OH}, k_3^B), indicates extensive rehybridization of the β carbon and is consistent with a concerted mechanism, with a transition state like 2 or possibly 3. As mentioned earlier, the positive deviation of the water reaction from the Brønsted plot (Figure 5) is another indication in favor of such a mechanism.

An alternative mechanism for the $k_{34}^{H_2O}$ step would be an unassisted rate-limiting breakdown of T_{OH}^0 into $PhCH{=}OH^+$ and Meldrum's acid anion which corresponds to specific acid catalysis in the reverse, addition direction. This mechanism was excluded based on a *solvent* kinetic isotope effect $k_{34}^{H_2O}/k_{34}^{D_2O} = 2.4$ in the case of T_{OH}^0 derived from 1,1-dinitro-2,2-diphenylethylene[6] and thus seems unlikely in the present case. Another possibility is a mechanism in which the hydronium ion formed by the deprotonation of the OH group of T_{OH}^0 is involved in hydrogen bonding to the developing carbonyl oxygen (preassociation mechanism in the reverse direction). Even though this mechanism cannot rigorously be excluded it has been shown to be much less satisfactory than the concerted one for 1,1-dinitro-2,2-diphenylethylene.[6] In the absence of additional evidence we therefore prefer the concerted mechanism also for the present case. We also note that **2** is analogous to the transition state postulated for water-catalyzed breakdown of nitrogen protonated carbinolamines[40] although Jencks now believes that the mechanism involving hydrogen bonding to the developing carbonyl oxygen is a distinct possibility.[41]

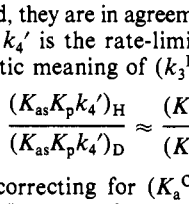

2

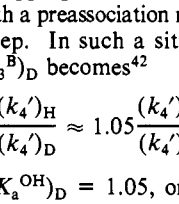

3

For the reactions of **1-H** and **1-OMe** the isotope effects on k_3^B for acetate and formate ion catalysis were determined in an analogous way as for **1-NO₂** (eq 13). Their values are 1.30 for **1-H** and 1.33 for **1-OMe**, i.e., much higher than those for **1-NO₂** and therefore inconsistent with a trapping mechanism. On the other hand, they are in agreement with a preassociation mechanism in which k_4' is the rate-limiting step. In such a situation the mechanistic meaning of $(k_3^B)_H/(k_3^B)_D$ becomes[42]

$$\frac{(k_3^B)_H}{(k_3^B)_D} = \frac{(K_{as}K_pk_4')_H}{(K_{as}K_pk_4')_D} \approx \frac{(K_a^{OH})_H}{(K_a^{OH})_D}\frac{(k_4')_H}{(k_4')_D} \approx 1.05\frac{(k_4')_H}{(k_4')_D} \quad (16)$$

After correcting for $(K_a^{OH})_H/(K_a^{OH})_D = 1.05$, one obtains $(k_4')_H/(k_4')_D = 1.24$ for **1-H** with both catalysts, 1.25 for **1-OMe** with acetate, 1.27 for **1-OMe** with formate ion.

From the intercepts of the buffer plots one could, in principle, determine the isotope effects on k_3^{OH} and $k_{34}^{H_2O}$ via eq 15 just as for **1-NO₂**. The values for $(k_{34}^{H_2O} + k_3^{OH}[OH^-])_H/(k_{34}^{H_2O} + k_3^{OH}[OH^-])_D$ summarized in Table V indeed show the expected trend toward a larger isotope effect at low pH where the $k_{34}^{H_2O}$ pathway becomes dominant and toward low values at high pH where the k_3^{OH} term is the major one. However, dominance of neither term is complete at any of the pH values investigated. Hence the isotope effects on k_3^{OH} and $k_{34}^{H_2O}$ had to be obtained by the potentially less accurate method of using the actual intercepts (rather than ratios) for the protio and deuterio compound, thereby obtaining the values of $(k_3^{OH})_H$, $(k_3^{OH})_D$, etc., separately. The results are as follows: $(k_3^{OH})_H/(k_3^{OH})_D = 1.03$ for both **1-H** and **1-OMe**; $(k_{34}^{H_2O})_H/(k_{34}^{H_2O})_D = 1.26$ for **1-H**, 1.24 for **1-OMe**. These values are, within experimental error, the same as for **1-NO₂** and therefore must have the same mechanistic meaning as for

(33) (a) Northcott, D.; Robertson, R. E. *J. Phys. Chem.* **1969**, *73*, 1559; (b) Van der Linde, W.; Robertson, R. E. *J. Am. Chem. Soc.* **1964**, *86*, 4505. (c) Halevi, E. A.; Nussim, M.; Ron, A. *J. Chem. Soc.* **1963**, 866. (d) Bary, Y.; Gilboa, H.; Halevi, E. A. *J. Chem. Soc., Perkin Trans. 2* **1979**, 938. (e) Bell, R. P.; Miller, W. B. T. *Trans. Faraday Soc.* **1963**, *59*, 1147. (f) Bell, R. P.; Crooks, J. E. *Ibid.* **1962**, *58*, 1409.

(34) (a) De Frees, D. J.; Bartmess, J. E.; Kim, J. K.; McIver, R. T., Jr.; Hehre, W. J. *J. Am. Chem. Soc.* **1977**, *99*, 6541. (b) De Frees, D. J.; Hassner, D. Z.; Hehre, W. J.; Peter, E. A.; Wolfsberg, M. *Ibid.* **1978**, *100*, 641.

(35) Shiner, V. J., Jr. In "Isotope Effects in Chemical Reactions"; Collins, C. J.; Bowman, N. S., Eds.; Van Nostrand-Reinhold: New York, 1970; p 90.

(36) (a) Okano, V.; do Amaral, L.; Cordes, E. H. *J. Am. Chem. Soc.* **1976**, *98*, 4201. (b) do Amaral, L.; Bastos, M. P.; Bull, H. G.; Cordes, E. H. *Ibid.* **1973**, *95*, 7369. (c) Young, P. R.; McMahon, P. E. *Ibid.* **1979**, *101*, 4678. (d) Palmer, J. L.; Jencks, W. P. *Ibid.* **1980**, *102*, 6472.

(37) Bilkadi, Z.; de Lorimier, R.; Kirsch, J. F. *J. Am. Chem. Soc.* **1975**, *97*, 4317.

(38) Knier, B. L.; Jencks, W. P. *J. Am. Chem. Soc.* **1980**, *102*, 6789.

(39) Formate ion catalysis, for which the deviation from the expected isotope effect is larger, was measured at pH < pK_1 which makes $(k_3^B)_H/(k_3^B)_D$ very sensitive to an error in K_1^H/K_1^D (eq 13); acetate ion catalysis was observed at pH values mostly above pK_1 where this sensitivity is low.

(40) (a) Rosenberg, S.; Silver, S. M.; Sayer, S. M.; Jencks, W. P. *J. Am. Chem. Soc.* **1974**, *96*, 7986. (b) Sayer, S. M.; Pinsky, B.; Schonbrunn, A.; Washtien, W. *Ibid.* **1974**, *96*, 7998.

(41) Jencks, W. P., personal communication.

(42) A more rigorous treatment gives $(k_3^B)_H/(k_3^B)_D = [(K_a^{OH})_H/(K_a^{OH})_D]^\delta(k_4')_H/(k_4')_D$ as will become apparent below, but numerically the two differ by not more than 1%.

Scheme II

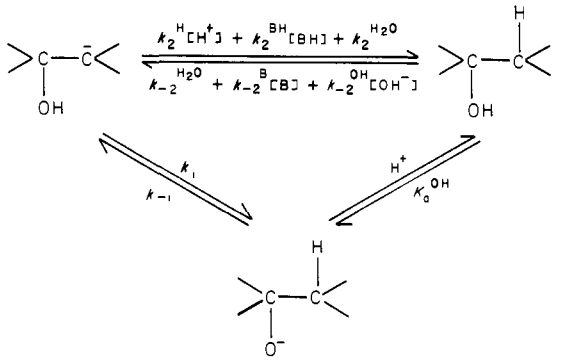

Table VI. Rate Constants for Reaction 2 of 1-H (Proton Transfer to and from Carbon) at 25 °C and μ = 0.5 M

k_2^H, M^{-1} s^{-1}	2.40×10^4 [a,b]
$k_{-2}^{H_2O}$, s^{-1}	27.2[a]
$k_{-2}^{H_2O}/k_2^H = K_a^{CH}(pK_a^{CH})$	1.12×10^{-3} (2.95)[a]
$k_2^{ClCH_2COOH}$, M^{-1} s^{-1}	1.26×10^3 [a]
$k_{-2}^{ClCH_2COO^-}$,[c] M^{-1} s^{-1}	4.45×10^2 [a]
$k_2^{MorH^+}$, M^{-1} s^{-1}	9.1×10^{-2}
k_{-2}^{Mor},[c] M^{-1} s^{-1}	6.15×10^4
$k_2^{HCO_3^-}$, M^{-1} s^{-1}	8.7×10^{-2}
$k_{-2}^{CO_3^{2-}}$,[c] M^{-1} s^{-1}	8.3×10^5
$k_2^{Et_3NH^+}$, M^{-1} s^{-1}	5.9×10^{-4}
$k_{-2}^{Et_3N}$,[c] M^{-1} s^{-1}	6.0×10^4
$(k_2^{H_2O} + k_i)/55$, M^{-1} s^{-1}	9.54×10^{-7}
$k_{-2}^{OH} + k_{-i}K_a^{OH}$,[d] M^{-1} s^{-1}	3.16×10^6

[a] From ref 3 in highly acidic solution. [b] $k_2^H = 2.6 \times 10^4$ is obtained from hydrolysis at pH 8.3; this work. [c] $k_{-2}^B = k_2^B K_a^{CH}/K_a^{BH}$; pK_a^{BH} = 2.50 ($ClCH_2COOH$), 8.78 ($MorH^+$), 9.93 (HCO_3^-), 10.96 (Et_3NH^+), 15.47 (H_2O).

1-NO_2: concerted water-catalyzed collapse of T_{OH}^0 for $k_{34}^{H_2O}$ and essentially encounter-controlled deprotonation of T_{OH}^0 by OH^- for k_3^{OH}. This latter conclusion implies that the preassociation mechanism does not manifest itself in the OH^--catalyzed reaction because k_a (or k_a and k_p; see above) rather than k_4' (Scheme I) is rate limiting.

Mechanism of Hydrolysis in Basic Solution: Proton Transfer to Carbon. The hydrolysis of **1-H** was investigated at pH ≥8.30 in morpholine, bicarbonate, and triethylamine buffers (Table S4[21]). In basic solution we have $k_3^{H_2O} + k_3^B[B] + k_3^{OH}[OH^-] \gg k_{-2}^{H_2O} + k_{-2}^B[B] + k_{-2}^{OH}[OH^-]$ and thus carbon protonation (eq 2) becomes rate limiting. At these pH values we also have pH ≫ pK_1; i.e., T_{OH}^- becomes the ground state and k_{obsd} is given by

$$k_{obsd} = k_2^H[H^+] + k_2^{BH}[BH] + k_2'^{H_2O} \qquad (17)$$

with $k_2'^{H_2O} = k_2^{H_2O} + k_i$; k_i refers to an intramolecular proton switch[43] (Scheme II) which might possibly compete with the intermolecular pathways. In bicarbonate buffers the plot of k_{obsd} vs. concentration is slightly curved (Figure 3) which is due to either nucleophilic attack on the olefin[1] or a change toward rate-limiting k_4'[44] or a combination of both. The phenomenon was not investigated further.

k_2^H, k_2^{BH}, and $k_2^{H_2O}$ are summarized in Table VI; k_2^{BH} for chloroacetic acid obtained by a different procedure in strongly acidic solution[3] is included in the table. We also note that $k_2^H = 2.6 \times 10^4$ M^{-1} s^{-1} is in excellent agreement with $k_2^H = 2.4 \times 10^4$ M^{-1} s^{-1} measured in HCl solutions.[3]

A Brønsted plot is shown in Figure 6. The correlation is not very good because experimental restrictions led us to use a rather heterogeneous group of catalysts: in acidic solution protonation on carbon was only detectable in a pH range appropriate for chloroacetic acid[3] while in the basic region catalysts which would not lead to nucleophilic attack on the olefin[1,3] had to be used. In order to "calibrate" our Brønsted plot we have therefore included Eigen's[4] data for the protonation of Meldrum's acid anion by H_3O^+, chloroacetic acid, benzoic acid, pyridinium ion, imidazolium ion, and phenol. The five buffer acids define a good Brønsted line with $\alpha = 0.49$. Assuming the same α value for protonation of T_{OH}^- we have drawn the dashed Brønsted line through the chloroacetic acid point (Figure 6). It is apparent that all other points deviate negatively from this line. The slight deviation for HCO_3^- is probably due to electrostatic repulsion[45] while the deviations for morpholinium ion and especially Et_3NH^+ must have a steric origin.

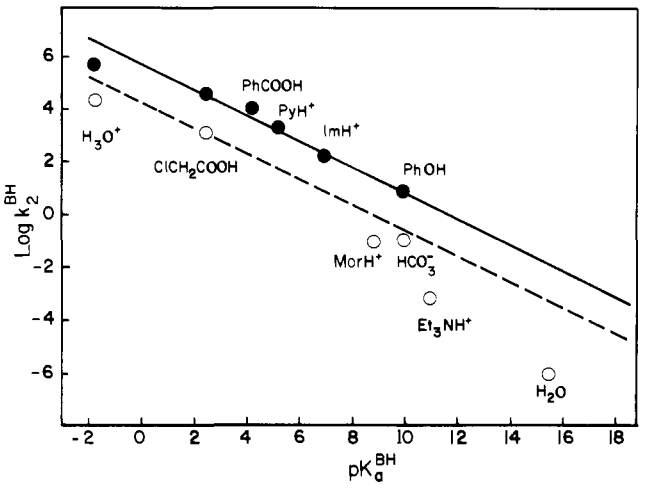

Figure 6. Brønsted plots for carbon protonation of T_{OH}^- (○, data from Table VI) and of Meldrum's acid anion (●, data from ref 4).

The deviations for the hydronium ion (≈6-fold) and for the water reaction (≈600-fold) are of the order of magnitude typical for such reactions.[45] This is an important conclusion because it shows that the water reaction is *not* unusually fast, indicating that k_i (Scheme II) at best contributes modestly or not at all. This result contrasts with observations pertaining to **4**[46] and similar

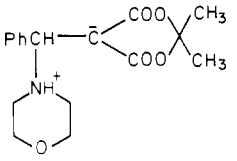

4

zwitterionic addition complexes[47] where intramolecular proton transfer is a major pathway; our result is, however, consistent with theoretical expectations.[48]

Estimates for k_4, k_4', and k_b. k_4 is only experimentally accessible for **1-NO_2** where it has a value of 5.4×10^9 s^{-1} (Table IV). If we assume that the Hammett ρ (ρ^+) value for the k_4 process is similar to that for cyanide ion departure from ArCH(O⁻)CN (ρ = −0.2 to −0.3),[36c,49] we can estimate $k_4 \approx 9 \times 10^9$ s^{-1} for **1-H**, $k_4 \approx 1.1 \times 10^{10}$ s^{-1} for **1-OMe**.

A different approach to estimating k_4 for these latter two compounds is based on k_3^B and the interdependence of k_4, k_4', and k_b; this interdependence is best appreciated as follows. Let us first assume that hydrogen bonding has *no* stabilizing influence on $T_{OH}^0 \cdot HB$ or on the transition state of the k_4' step (Scheme I). This would mean that $k_4' = k_4$. It would further imply that the k_b step refers to the diffusional separation of two species which do not interact and for which we shall assume $k_b^0 = 5 \times 10^{11}$ s^{-1}.[50]

(43) The transition state is likely to contain one (or more) water molecule(s).

(44) $k_3^{OH} \gg k_{-2}^{OH}$ but $k_3^{CO_2^{2-}} \ll k_{-2}^{CO_3^{2-}}$. Hence when the buffer term becomes dominant there is a change in the rate-limiting step.

(45) Kresge, A. J. *Chem. Soc. Rev.* **1973**, *2*, 475.
(46) Bernasconi, C. F.; Fornarini, S. *J. Am. Chem. Soc.* **1980**, *102*, 5329.
(47) Bernasconi, C. F.; Carrè, D. J. *J. Am. Chem. Soc.* **1979**, *101*, 2698.
(48) Bernasconi, C. F.; Hibdon, S. A.; McMurry, S. E. *J. Am. Chem. Soc.* **1982**, *104*, 3459.
(49) Ching, W.-M.; Kallen, R. G. *J. Am. Chem. Soc.* **1978**, *100*, 6119.

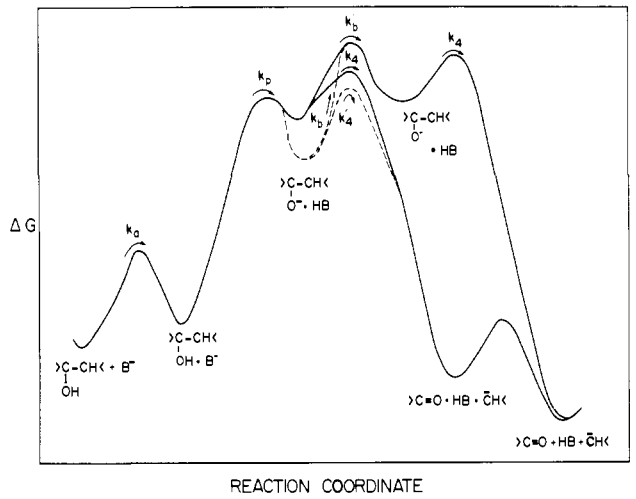

Figure 7. Free energy–reaction coordinate diagram for conversion of T_{OH}^0 into benzaldehyde and Meldrum's acid anion catalyzed by a weak base (thermodynamically unfavorable proton transfer). Upper solid line shows trapping mechanism, lower solid line preassociation mechanism, both without hydrogen bonding. Upper dashed line refers to trapping mechanism with hydrogen bonding stabilization of the intermediate; lower dashed line shows the preassociation mechanism with hydrogen bonding in the intermediate and in the transition state.

This situation is represented by the solid lines in Figure 7. For the trapping mechanism the rate constant would thus be given by $k_3^B = K_{as}K_p^0k_b^0$, for the preassociation by $k_3^B = K_{as}K_p^0k_4$ ($k_4'^0 = k_4$); the zero superscript indicates absence of hydrogen bonding, K_p^0 is defined by K_a^{OH}/K_a^{BH}, while $K_{as} = 0.02$.[51]

Now let us assume that T_{OH}^{0-}·HB *is* stabilized by hydrogen bonding as indicated by the dashed lines in Figure 7. In as much as there is still hydrogen bonding in the transition state of the k_4' step, its energy is also lowered but by less than that of T_{OH}^{0-}·HB (lower dashed line). The net effect is to reduce k_4' so that now $k_4' < k_4$. For the k_b step no transition state[52] stabilization is assumed (upper dashed line) and k_b is reduced by an amount which is equivalent to the stabilization of T_{OH}^{0-}·HB. In quantitative terms we have now $k_3^B = K_{as}K_pk_b$ for the trapping, $k_3^B = K_{as}K_pk_4'$ for the preassociation mechanism, but here $K_p = (K_p^0)^{\beta_p} = (K_a^{OH}/K_a^{BH})^{\beta_p}$, $k_b = k_b^0(K_a^{OH}/K_a^{BH})^{\beta_b}$, and $k_4' = k_4(K_a^{OH}/K_a^{BH})^{\beta'}$.

The experimental β values can be equated with $\beta_p + \beta'$ in the case of the preassociation mechanism (0.82 average of β for **1-H** and **1-OMe**) while for the trapping mechanism (**1-NO$_2$**) $\beta = 1.0 = \beta_p + \beta_b$. We can draw two conclusions from this. (a) Since $\beta_p + \beta' \approx 0.82$, this implies $\beta_p \leq 0.82$. (b) Since $\beta_p + \beta_b = 1.0$, the expression $K_{as}K_pk_b$ is equivalent to $K_{as}K_p^0k_b^0$; i.e., the energy of the transition state of the trapping mechanism is indeed unaffected by hydrogen bonding, as assumed (Figure 7).

Estimates for β_p, β_b, and β' can be obtained based on the Hine[53] equation for the association constant of a hydrogen bond donor (HA) with an acceptor (B^-) in aqueous solution.

$$\log K_{AB} = \tau(pK_{HA} - pK_{H_2O})(pK_{H_3O^+} - pK_{BH}) - 1.74 \qquad (18)$$

If we equate K_{AB} with k_{-b}/k_b and assume hydrogen bonding affects only k_b ($k_{-b} = 10^{10}$ M^{-1} s^{-1}), we can calculate k_b as $k_{-b}/K_{AB} = 10^{10}/K_{AB}$. β_b is then obtained as $\log (k_b/5 \times 10^{11})/\log (K_a^{OH}/K_a^{BH})$ and further $\beta_p = 1.0 - \beta_b$ and $\beta' = \beta - \beta_p$. In the case of **1-NO$_2$** we use the experimental k_4 to calculate $k_4' = k_4(K_a^{OH}/K_a^{BH})^{\beta'}$ while for **1-H** and **1-OMe** one obtains k_4' from k_3^B as $k_4' = k_3^B/K_{as}(K_a^{OH}/K_a^{BH})^{\beta_p}$ with $K_{as} = 0.02$;[54] k_4 is calculated as $k_4 = k_4'/(K_a^{OH}/K_a^{BH})^{\beta'}$.

Table VII. Estimates for k_4, k_4', and k_b Based on the Hine Equation[d]

	$B^- = AcO^-$ ($pK_a^{BH} = 4.57$)	$B^- = HCOO^-$ ($pK_a^{BH} = 3.46$)
A. 1-NO$_2$ ($pK_a^{OH} = 13.65$)		
K_{AB}	3.16	5.23
$k_b = 10^{10}/K_{AB}$	3.17×10^9	1.91×10^9
$\beta_b = \log (k_b/5 \times 10^{11})/\log (K_a^{OH}/K_a^{BH})$	0.241	0.238
$\beta_p = 1.00 - \beta_b$	0.759	0.762
$\beta' = \beta - \beta_p$ ($\beta = 0.82^a$)	0.061	0.058
$k_4' = k_4(K_a^{OH}/K_a^{BH})^{\beta'}$	1.50×10^9	1.38×10^9
k_4	5.40×10^9 [b]	5.40×10^9 [b]
B. 1-H ($pK_a^{OH} = 14.45$)		
K_{AB}	4.09	7.10
$k_b = 10^{10}/K_{AB}$	2.45×10^9	1.41×10^9
$\beta_b = \log (k_b/5 \times 10^{11})/\log (K_a^{OH}/K_a^{BH})$	0.234	0.232
$\beta_p = 1.00 - \beta_b$	0.766	0.768
$\beta' = \beta - \beta_p$ ($\beta = 0.82^c$)	0.054	0.052
k_3^B	2.82	0.33
$k_4' = k_3^B/K_{as}(K_a^{OH}/K_a^{BH})^{\beta_p}$	5.50×10^9	4.69×10^9
$k_4 = k_4'/(K_a^{OH}/K_a^{BH})^{\beta'}$	1.88×10^{10}	1.74×10^{10}
C. 1-OMe ($pK_a^{OH} = 14.70$)		
K_{AB}	4.37	7.68
$k_b = 10^{10}/K_{AB}$	2.29×10^9	1.30×10^9
$\beta_b = \log (k_b/5 \times 10^{11})/\log (K_a^{OH}/K_a^{BH})$	0.231	0.230
$\beta_p = 1.00 - \beta_b$	0.769	0.770
$\beta' = \beta - \beta_p$ ($\beta = 0.82^c$)	0.051	0.050
k_3^B	2.31	0.31
$k_4' = k_3^B/K_{as}(K_a^{OH}/K_a^{BH})^{\beta_p}$	7.25×10^9	6.93×10^9
$k_4 = k_4'/(K_a^{OH}/K_a^{BH})^{\beta'}$	2.38×10^{10}	2.51×10^{10}

[a] Based on the assumption that if 1-NO$_2$ were hydrolyzed by a preassociation mechanism it would have the same β value as **1-H** and 1-OMe. [b] Experimentally determined. [c] Average of β for 1-H and 1-OMe. [d] Equation 18 using $\tau = 0.013$; see text.

The various parameters are summarized in Table VII. They are based on $\tau = 0.013$ (eq 18), a value suggested by Jencks.[55] The picture which emerges is consistent with our mechanistic conclusions as well as with "reasonable expectations".

(1) For **1-NO$_2$** $k_b > k_4'$ for both catalysts which is consistent with the trapping mechanism. Note, however, that k_b exceeds k_4' by only 1.5-fold for formate ion, by 2.1-fold for acetate ion catalysis. This suggests some competition by the preassociation mechanism and could explain why the isotope effects are somewhat larger than expected for a pure trapping mechanism, particularly for formate ion catalysis.[56]

(2) For **1-H** and **1-OMe** $k_4' > k_b$ for both catalysts as required for the preassociation mechanism. The k_4'/k_b ratios are not very large (2.25 for **1-H**/AcO$^-$, 3.32 for **1-H**/HCOO$^-$, 3.17 for **1-OMe**/AcO$^-$, 5.32 for **1-OMe**/HCOO$^-$) and suggest some competition by the trapping mechanism. The slightly smaller isotope effects for **1-H** on k_4' for **1-H** (1.30/1.05 = 1.24) compared to **1-OMe** (1.25 and 1.28), if significant at all, would be consistent with the slightly larger contribution by the trapping mechanism in the **1-H** reactions.

(3) The increase in k_4'/k_b in the direction **1-NO$_2$** → **1-H** → **1-OMe** is mainly due to an increase in k_4' (more push by electron-donating substituent) but there is also a small decrease in

(50) Experimental values of this order of magnitude have been reported for noninteracting complexes;[7] a similar value is obtained by assuming an encounter rate constant $k_{-b} \approx 10^{10}$ and an association equilibrium constant of 0.017 ($=k_{-b}/k_b$) estimated by Hine;[28] our assumption implies $k_{-b}/k_b = 0.02$ (with $k_{-b} = 10^{10}$).[51]

(51) T_{OH}^0·B is assumed to be an encounter complex for which hydrogen-bonding stabilization is insignificant, with $k_a = 10^{10}$ M^{-1} s^{-1}, $k_{-a} = 5 \times 10^{11}$ s^{-1}.

(52) The term "transition state" has obviously a somewhat different meaning in a diffusional process.

(53) Hine, J. *J. Am. Chem. Soc.* **1972**, *94*, 5766.

(54) Application of the Hine equation to K_{as} for T_{OH}^0·B shows a negligible effect of hydrogen bonding, as assumed earlier (ref 51).

(55) Funderburk, L. H.; Jencks, W. P. *J. Am. Chem. Soc.* **1978**, *100*, 6708.

(56) If there was competition by the preassociation mechanism the plateaus in Figure 2 should not be completely horizontal. The fact that they are essentially horizontal could mean (1) that the estimated k_b is somewhat too small and/or the estimated k_4' value somewhat too large, or (2) that the rather high concentration of the buffer acid (>1 M) at the higher buffer concentration reduces k_{obsd} slightly by a medium effect.

k_b due to increased hydrogen bonding to the more basic oxyanion.

(4) The values for β_b, β_p, and β' seem reasonable. In particular $\beta_p < \beta$ as required; β' values of 0.05 to 0.06 indicate that hydrogen bonding in the transition state of the k_4' step is only slightly less than in T_{OH}^{0-}·HB; i.e., the transition state resembles the complex which is consistent with a relatively small ρ value (see below).

We wish to stress that the parameters in Table VII should not be taken too literally. They depend on the relatively arbitrary choice of a τ value (eq 18); a slightly different τ would lead to a somewhat different set of parameters with an equally satisfactory internal consistency. On the other hand, if Hine's τ value of 0.024[53] were chosen, the parameters in Table VII would take on some rather unrealistic values. For example for **1-NO$_2$**/AcOH we would obtain $K_{AB} = 240$, $k_b = 4.16 \times 10^7$ s^{-1}, $\beta_b = 0.45$, $\beta_p = 0.55$, $\beta' = 0.27$ and $k_4' = 1.70 \times 10^7$ s^{-1}. That β_b should be almost as large as β_p makes little sense. We therefore believe that our data serve as an indirect method to show that Jencks' $\tau = 0.013$[55] is a reasonable value.

Incidentally the addition of thiolate ions to acetaldehyde reported by Jencks and Gilbert[12] shows many of the same characteristics as our reactions and they have been discussed in a somewhat similar way.

Isotope Effects and ρ Values. A. k_4 and k_4'. The collapse of intermediates such as ArCH(O$^-$)X or ArCH(OH)X with X$^{(-)}$ = RS$^-$, OH$^-$, CN$^-$, or RNH$_2$ is usually associated with a very small α secondary kinetic deuterium isotope effect ($\approx$1.05 or less) while the equilibrium isotope effect is typically in the order of 1.24 to 1.39.[36a-c,57,58] This suggests a transition state in which sp^3 → sp^2 rehybridization has made only very little progress.[35-38] The smallness of the ρ or normalized ρ values usually observed for the collapse rates[36c,40a,49] is consistent with this view.

In contrast to that, our kinetic isotope effects on the k_4 step for **1-NO$_2$** (1.20) or on the k_4' steps for **1-H** (1.24) and **1-OMe** (1.25, 1.28) are very large. If the equilibrium isotope effects are also in the range of 1.24 to 1.39 which seems a reasonable assumption, these results would suggest extensive (> (≫) 50%) sp^3 → sp^2 rehybridization in the transition state.

A correlation of the k_4 and k_4' with the standard σ values affords $\rho = -0.63$ (k_4) and $\rho = -0.67$ (k_4'). Since k_4 for **1-H** and **1-OMe**, and k_4' for **1-NO$_2$** were obtained based on the Hine equation (eq 18) and therefore represent only estimates, it could be argued that not much significance should be attached to these ρ values. However, even though the *absolute* values of the k_4 and k_4' estimates depend greatly on the assumed τ values in eq 18, their *relative* values show only a very small dependence on τ. For example, k_4'(**1-OMe**)/k_4'(**1-NO$_2$**) = 4.83 for acetate ion catalysis when $\tau = 0.013$ (Table VII); if $\tau = 0.024$ were assumed instead, the absolute values of k_4' would be lowered about 100-fold but k_4'(**1-OMe**)/k_4'(**1-NO$_2$**) = 3.84 changes by only 20% and ρ would change by less than 0.08.

The observed ρ values are significantly larger (more negative) than the value of −0.22 for the rate of cyanide ion loss from ArCH(O$^-$)CN,[49] suggesting a more advanced transition state than for cyanide ion loss. If ρ_{eq} for the equilibrium constant for Meldrum's acid anion loss were comparable to $\rho_{eq} = -1.92$ for cyanide ion loss,[49] a normalized ρ value (ρ/ρ_{eq}) of −0.30 to −0.35 would reslt, suggesting that C–C bond breaking is 30 to 35% complete in the transition state. This conclusion contrasts with that drawn from the isotope effects which suggested a late transition state. This apparent contradiction might have a number of causes.

(1) The equilibrium isotope effect on our reaction could be much larger than that for similar reactions reported in the literature and/or ρ_{eq} might be much smaller than assumed. We cannot disprove this hypothesis but we do not see good reasons why this should be the case.

(2) The commonly made assumption that the kinetic isotope effect and the normalized ρ value measure the same transition-state property may not be justified. Recent studies by Knier and Jencks,[38] and by Pohl and Hupe[59] suggest that the nature of the nucleophile (nucleofuge) can have a dramatic effect on secondary kinetic isotope effects which does not seem to correlate with other transition-state parameters. These studies show that polarizable nucleophiles (nucleofuges) such as thiolate ions and others lead to larger kinetic isotope effects when the reaction is in the direction sp^3 → sp^2. A highly delocalized carbanion such as Meldrum's acid anion in our reaction could possibly behave in the same manner.

(3) The discrepancy between the kinetic isotope effect and ρ might indicate an imbalance in the transition state; this could come about if during C–C bond cleavage there is first some localization of negative charge on carbon (**5**) which only later is being delocalized into the product Meldrum's acid anion. This is directly analogous to one of the current explanations[60-62] of the nitroalkane anomaly[63] (eq 20). According to this interpretation the isotope effect would perhaps be a relatively reliable measure of the degree of sp^3 → sp^2 rehybridization and with it of the degree of C–C bond cleavage in the transition state; ρ would not be such a measure because the close proximity of the partial negative charge on carbon renders ρ less negative than it would be if this charge were already delocalized into the (COO)$_2$C(CH$_3$)$_2$ moiety.

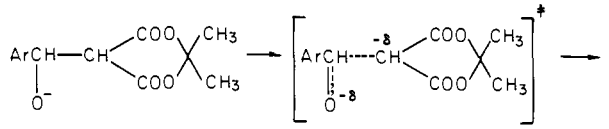

5

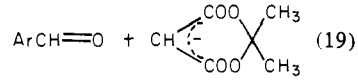

(19)

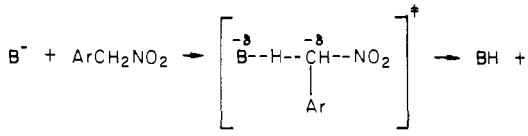

ArCH=NO$_2^-$ (20)

We cannot, at the present time, make a clear distinction between interpretations 2 and 3. They might actually be related. We note, however, that the notion of an imbalanced transition state associated with the strongly delocalizing (COO)$_2$C(CH$_3$)$_2$ moiety is consistent with similar imbalances found in the nucleophilic addition to substituted benzylidene Meldrum's acids.[1,46] This would add another member to a growing list of imbalanced transition states.[64]

B. Concerted Pathway, $k_{34}^{H_2O}$. $k_{34}^{H_2O}$ correlates well with the standard σ values, with $\rho = -1.60$. This ρ value is about as large as ρ_{eq} for the equilibrium constant of HCN loss from ArCH(OH)CN[49] and suggests a very late transition state. The large kinetic isotope effects on $k_{34}^{H_2O}$ (1.24 and 1.26, footnotes *c* and *d* in Table VII) which are close to the *equilibrium* isotope effect for the collapse of ArCH(OH)CN (1.28[36a]) lead to the same conclusion.

One wonders then why in the water-catalyzed breakdown of T_{OH}^0 the isotope effects and the ρ value give a consistent picture of the transition state while in the collapse of T_{OH}^{0-} these measures lead to contradictory conclusions. If, as suggested above, there is a transition-state imbalance in the latter reaction which is due to a localization of negative charge on the α carbon (**5**), such imbalance would be expected to be less pronounced or to disappear

(57) Lewis, C. A.; Wolfenden, R. *Biochemistry* **1977**, *16*, 4886.
(58) Hill, E. A.; Milosevich, S. A. *Tetrahedron Lett.* **1976**, 4553.
(59) Pohl, E. R.; Hupe, D. J. *J. Am. Chem. Soc.* **1980**, *102*, 2763.
(60) Kresge, A. J. *Can. J. Chem.* **1974**, *52*, 1897.
(61) Jencks, D. A.; Jencks, W. P. *J. Am. Chem. Soc.* **1977**, *99*, 7948.
(62) Keeffe, J. R.; Morey, J.; Palmer, C. A.; Lee, J. C. *J. Am. Chem. Soc.* **1979**, *101*, 1295.
(63) (a) Fukuyama, M.; Flanagan, P. W. K.; Williams, F. T., Jr.; Frainier, L.; Miller, S. A.; Schechter, H. *J. Am. Chem. Soc.* **1970**, *92*, 4689. (b) Bordwell, F. G.; Boyle, W. J., Jr. *Ibid.* **1972**, *94*, 3907. (c) Bordwell, F. G.; Boyle, W. J., Jr. *Ibid.* **1975**, *97*, 3447. (d) Bordwell, F. G.; Bartmess, J. E.; Hautala, J. A. *J. Org. Chem.* **1978**, *43*, 3107.
(64) For a partial list see ref 1.

in the reaction of T_{OH}^0 because this negative charge is (partially) compensated by the positive charge on water (2) or by protonation (3).

Another factor which could reduce the imbalance in the transition state of the water-catalyzed reaction is that in general a very late transition state is less likely to be strongly imbalanced. This is best visualized if one places the reaction coordinate on a diagram with separate axes for C–C bond cleavage and for charge delocalization. As the reaction coordinate approaches the product corner, it inevitably also approaches the diagonal line for balanced reactions. If the larger secondary isotope effects for the water reaction (1.24 to 1.28) compared to that of the k_4 step (1.20) is a true indication of a later transition state, this factor could be significant.

C. Water Addition to the Double Bond, K_1. We note that the equilibrium isotope effect on K_1 (average $K_1^H/K_1^D = 0.906$) is substantially smaller than the equilibrium isotope effects for nucleophilic addition to carbonyl carbon.[36,57,58] Whether this is typical for the addition to activated olefins will have to await further study. Nevertheless, it is noteworthy that this result is consistent with expectations based on fractionation factor calculations.[65]

Experimental Section

Materials. 1-H, 1-NO_2, and **1-OMe** were available from a previous study.[1] The deuterated analogues were synthesized by condensation of Meldrum's acid with the respective deuterated benzaldehyde as described by Schuster et al.;[66] the isotopic purity of the deuterated olefins was 98% or better as shown by NMR analysis. Benzaldehyde-d_1 was prepared by the method of Schowen et al.,[67] *p*-methoxylbenzaldehyde-d_1 by the method of Vitullo et al.,[68] *p*-nitrobenzaldehyde-d_1 by a modification[21] of Kirby's[69] procedure.

Morpholine and triethylamine were purified by refluxing for 8 h over sodium followed by distillation under nitrogen. The other materials were all reagent grade and were used without further purification.

Equilibrium Measurements. K_1^H and K_1^D were measured spectrophotometrically at λ_{max} of the olefin (325 nm for 1-H, 320 nm for **1-NO_2**, 372 nm for **1-OMe**); at these wavelengths T_{OH}^- does not absorb. pK_1 was obtained as

$$pK_1 = pH + \log \frac{OD}{OD_0 - OD} \quad (21)$$

where OD refers to the optical density at a pH close to pK_1 while OD_0 is the optical density of a solution where all the material is in the olefin form. Since the solutions were unstable owing to the onset of the hydrolysis reaction, the following procedure was adopted. A few microliters of a stock solution of the olefin in Me_2SO as injected into a prethermostated buffer solution placed into a cuvette of a Gilford spectrophotometer. The OD was recorded as a function of time with the time of injection being $t = 0$. Logarithmic plots of ΔOD vs. time where extrapolated to $t = 0$ in order to obtain the desired OD.

Kinetic Experiments. The techniques used were the same as the ones reported before.[1,3]

Acknowledgment. This research was supported by Grant CHE80-24261 from the National Science Foundation. We wish to thank Professor William P. Jencks for criticisms and suggestions.

Registry No. 1-H, 1214-54-6; 1-NO_2, 15795-62-7; **1-OMe**, 15795-54-7.

Supplementary Material Available: Tables S1–S4, observed rate constants for hydrolytic cleavage of **1-NO_2** and **1d-NO_2** (S1), of **1-H** and **1d-H** (S2), and of **1-OMe** and **1d-OMe** (S3); observed rate constants for hydrolytic cleavage of **1-NO_2**, **1-H**, and **1-OMe**, additional data (S4); synthesis of *p*-nitrobenzaldehyde-d_1 (9 pages). Ordering information is given on any current masthead page.

(65) (a) Hartshorn, S. R.; Shiner, V. J., Jr. *J. Am. Chem. Soc.* **1972**, *94*, 9002. (b) Gray, C. H.; Coward, J. K.; Schowen, B.; Schowen, R. L. *Ibid.* **1979**, *101*, 4351.

(66) Schuster, P.; Polanski, O. E.; Wessely, F. *Monatsch. Chem.* **1964**, *95*, 53.

(67) Burgstahler, A. W.; Walker, D. E., Jr.; Kuebrich, J. P.; Schowen, R. L. *J. Org. Chem.* **1972**, *37*, 1272.

(68) Vitullo, V. P.; Wilgis, F. P. *J. Am. Chem. Soc.* **1981**, *103*, 880.

(69) Bennett, D. J.; Kirby, G. W.; Moss, V. A. *J. Chem. Soc., Chem. Commun.* **1967**, 218.

Reactivity of Some Transition-Metal Systems toward Liquid Carbon Dioxide

Michael G. Mason and James A. Ibers*

Contribution from the Department of Chemistry, Northwestern University, Evanston, Illinois 60201. *Received December 28, 1981*

Abstract: The reactivity of several transition-metal complexes toward liquid CO_2 has been investigated as a means of screening such complexes for their ability to bind CO_2. Although the known $Ni(CO_2)(PCy_3)_2$ complex was prepared by the reaction of $[Ni(PCy_3)_2]_2(\mu\text{-}N_2)$ with $CO_2(l)$, the compounds $Pd(PCy_3)_2$ and $Pt(PCy_3)_2$ do not react with $CO_2(l)$ to afford CO_2 complexes. But the compound $Pt(PCy_3)_2$ does react with wet CO_2 to afford $PtH(O_2COH)(PCy_3)_2$, a bicarbonato complex. Similar reactivity was seen for $W(CO)_3(PCy_3)_2$, which produces $WH(O_2COH)(CO)_3(PCy_3)_2$ in wet $CO_2(l)$. The compounds $Na[Co(N_2)(PEt_2Ph)_3]$ and $[Co(PEt_2Ph)_3]_2(\mu\text{-}N_2)$ react with $CO_2(l)$ to form complexes that contain carbonyl and carbonato ligands. Peroxocarbonato complexes, $IrR(OCO_3)(CO)(PPh_3)_2$ (R = Me, Ph), were prepared from $IrR(O_2)(CO)(PPh_3)_2$ with $CO_2(l)$.

Carbon dioxide offers an attractive potential alternative to carbon monoxide in the development of a C_1 chemical technology to supplement present petroleum-based technology. Before such a development can be realized, transition-metal–carbon dioxide interactions must be studied, as it is presumed that the catalytic reduction of carbon dioxide, if it is to be accomplished at all, will be carried out in the presence of a transition metal.[1]

Eisenberg and Hendriksen[1] recently reviewed the coordination chemistry of carbon dioxide and summarized some examples of metal complexes originally believed to be those of carbon dioxide that on further examination turned out to be otherwise. Because of difficulties of spectroscopic characterization, the unpredictable effects of adventitious water, and the tendency of coordinated CO_2 to react further, it is prudent to accept structural characterization by diffraction methods as the criterion for judging the authenticity of a given class of transition-metal–carbon dioxide complexes

(1) Eisenberg, R.; Hendriksen, D. E. *Adv. Catal.* **1979**, *28*, 119–144.

0002-7863/82/1504-5153$01.25/0